

The Oxidation State of Iron at High Pressure

Fe(III) reduces to Fe(II) in solids at high pressure;
the process is reversible.

H. G. Drickamer, G. K. Lewis, Jr., S. C. Fung

I. Introduction

Mössbauer resonance is a convenient tool for studying the electronic behavior of iron in various environments. High pressure Mössbauer studies in this laboratory (1-7) have shown that, in a wide variety of compounds, ferric ion reduces to the ferrous state with increasing pressure, and that this is a reversible process. Before describing and analyzing these results, it will be useful to review briefly the relevant features of the Mössbauer effect, to outline some aspects of ligand field and molecular orbital theory and to mention the results of some high pressure optical studies which will be helpful in the interpretation of the experiments discussed in this paper.

II. Mössbauer Resonance

There are available excellent expositions of the principles of Mössbauer resonance (8, 9) so that we confine ourselves to a short discussion of those features important in determining the oxidation state of iron. When a free atom decays emitting a gamma ray, it recoils to conserve momentum. As a result of energy conservation, the energy of the emitted gamma ray no longer corresponds exactly to that of

the nuclear transition, and, in addition, the energy spectrum is Doppler broadened. A similar argument applies to the absorption of a gamma ray by a free atom. If the atom is fixed in a crystal where the lowest quantum of vibrational energy (lowest phonon energy) is large compared to the recoil energy, an appreciable fraction of the decays are recoilless. Since the atom vibrates around an equilibrium position, the peak is not Doppler broadened and presents a very nearly monochromatic measure of the energy difference between the ground and the excited states of the nucleus. This difference (the isomer shift) is measurably affected by the electronic wave functions having non-zero amplitude at the nucleus (*s* electrons). Changes in the environment are reflected in the isomer shift through changes in occupation of the *4s* levels and changes in the degree of shielding of the *3s* orbitals by the *3d* electrons. The ferrous ion nominally has six *3d* electrons and the ferric ion five. Therefore these two states typically exhibit distinctly different isomer shifts and are easily distinguishable in a Mössbauer spectrum.

An electric field gradient at the nucleus interacts with the nuclear quadrupole moment to split the state of spin 3/2 and give two peaks in the spectrum. In the usual "ionic" complex, according to Hund's rule, the *3d* states are occupied in a manner which gives maximum multiplicity (high spin).

The aspherical distribution of the six electrons of the ferrous ion gives a significant electric field gradient at the nucleus, and thus a large quadrupole splitting. The spherically symmetric ferric state exhibits small quadrupole splitting. This effect also helps to distinguish the two states.

In very covalent compounds with a very strong ligand field, such as potassium ferricyanide the iron ions tend to pair their spins. For these low spin materials, the difference between the Mössbauer spectra of the ferrous and ferric states is less spectacular, but the determination can still be made. In the first order, the relative areas under the two sets of peaks give a reasonable measure of the amounts of ferrous and ferric ion present.

III. Transition Metal Ions in Crystals

The energy states of a *3d* electron on a free transition metal ion are fivefold degenerate. The separation between the ground and excited states is due to the repulsion among the *3d* electrons, and can conveniently be expressed in terms of the Racah parameters *A*, *B*, and *C* which we here consider as established empirically. When the ion is placed in a crystal where the field is less than spherically symmetric, the degeneracy is partially removed. We shall phrase this discussion in terms of an octahedral field, although the ideas are not qualitatively different for other symmetries. [Nor is the reduction of Fe(III) to Fe(II) which is the main theme of this paper.] The *3d* levels split into two states, a triply degenerate level labeled *t_{2g}* and a doubly degenerate level of higher energy labeled *e_g*. The energy difference is commonly called 10 Dq or Δ . Optical absorption peaks of moderately low intensity in the near infrared and visible spectrum measure 10 Dq as well as the values of *B* and *C* in the crystal. These latter parameters are generally lower in the crystal than in the free ion by an amount that depends on the type of ligand. With pressure, the crystal field parameter 10 Dq increases because of the increased field of the ligands, roughly as predicted by

The authors are associated with the department of Chemistry and Chemical Engineering and the Materials Research Laboratory, University of Illinois, Urbana 61801.

theory. The Racah parameters B and C decrease with increasing pressure. This can be attributed to spreading of the $3d$ orbitals, including an outward movement of the radial maximum, which reduces the interelectronic repulsion. We shall refer to this phenomenon in our later discussion.

Generally, energy levels in a complex can be best described in terms of a molecular orbital diagram as shown in Fig. 1. The predominantly metallic antibonding levels t_{2g} and e_g , as well as their separation $10Dq$, are marked. As shown, it is possible for the t_{2g} orbital to form a pi bond with excited ligand orbitals which tends to stabilize it (i.e., lower its energy) by a modest amount. This fact will also be of use to us later.

In addition to the absorption peaks mentioned above, there appear very intense peaks centered at about 3–4 eV ($24,000$ – $32,000$ cm^{-1}), with tails which may extend through the visible region. These correspond to ligand-to-metal charge transfer. In Fig. 1 such transfer is indicated from the non-bonding

ligand t_{2u} level to the metallic t_{2g} state. These peaks shift to lower energy by as much as an electron volt in 100 kilobars. There are at least two apparent causes for this red shift. In the first place, the pi bonding tends to increase with pressure faster than the sigma bonding, lowering the energy of the t_{2g} level vis-à-vis the ligand levels. The calculations of Lewis (3) show that this is a factor, but probably not the dominant one. In the second place, the spreading of the $3d$ electrons mentioned above lowers the energy of the $3d$ states substantially. This, in fact, is probably the major contribution (3, 10).

IV. The Reduction of Ferric Ion

As mentioned in the introduction, it has been found that the reversible reduction of Fe(III) to Fe(II) with increasing pressure is an ubiquitous phenomenon. We shall discuss first a few examples, together with an analy-

sis of the process, and then present some special cases of unusual interest.

Fig. 2 shows conversion data for FeCl_3 , FeBr_3 , and KFeCl_4 . The first two compounds have slightly distorted octahedral symmetry, while in KFeCl_4 the iron is in a tetrahedral site. The equilibrium constant

$$K = \frac{C_{\text{II}}}{C_{\text{III}}}$$

where C_{II} and C_{III} are the concentrations of Fe(II) and Fe(III) sites including the ligands. The linear relationship between $\ln K$ and $\ln P$ is very general. Constants A and B for the equation $K = AP^B$ are listed in Table 1 for a large number of compounds. There is clear evidence that these results represent equilibrium and not the result of slow kinetics. In the first place, consecutive runs at the same pressure gave essentially identical results. In the second place, when pressure was increased, as soon as a spectrum became resolved on the oscilloscope (5–15 minutes) the increased conversion was evident and remained constant with time, although complete runs took 8–48 hours or longer.

One can present a straightforward thermodynamic analysis:

$$K = \exp\left(-\frac{\Delta\bar{G}}{RT}\right) \quad (1)$$

$$\frac{\partial \ln K}{\partial \ln P} = \frac{P\Delta\bar{V}}{RT} = \frac{P(\bar{V}^{\text{III}} - \bar{V}^{\text{II}})}{RT} = B \quad (2)$$

where \bar{V}^{III} and \bar{V}^{II} represent the partial molar volumes of the Fe(III) and Fe(II) ions with their associated ligands. A slight rearrangement of Eq. 2 gives:

$$\frac{\partial \ln C_{\text{II}}}{\partial \ln P} = \frac{P(\bar{V}^{\text{III}} - \bar{V}^{\text{II}})}{RT} C_{\text{III}} \quad (3)$$

The fractional increase in concentration of reduced sites per fractional increase in pressure is proportional to the concentration of sites available for conversion. The coefficient of proportionality is the work to convert a site measured in thermal units (units of RT). It is perhaps surprising that this is independent of pressure, i.e., that the volume change accompanying reduction is inversely proportional to the pressure, and this may be true only within our limits of accuracy. The pressure range over which its validity has been established is 10–200 kilobars. Also, conversions less than 6–7% or

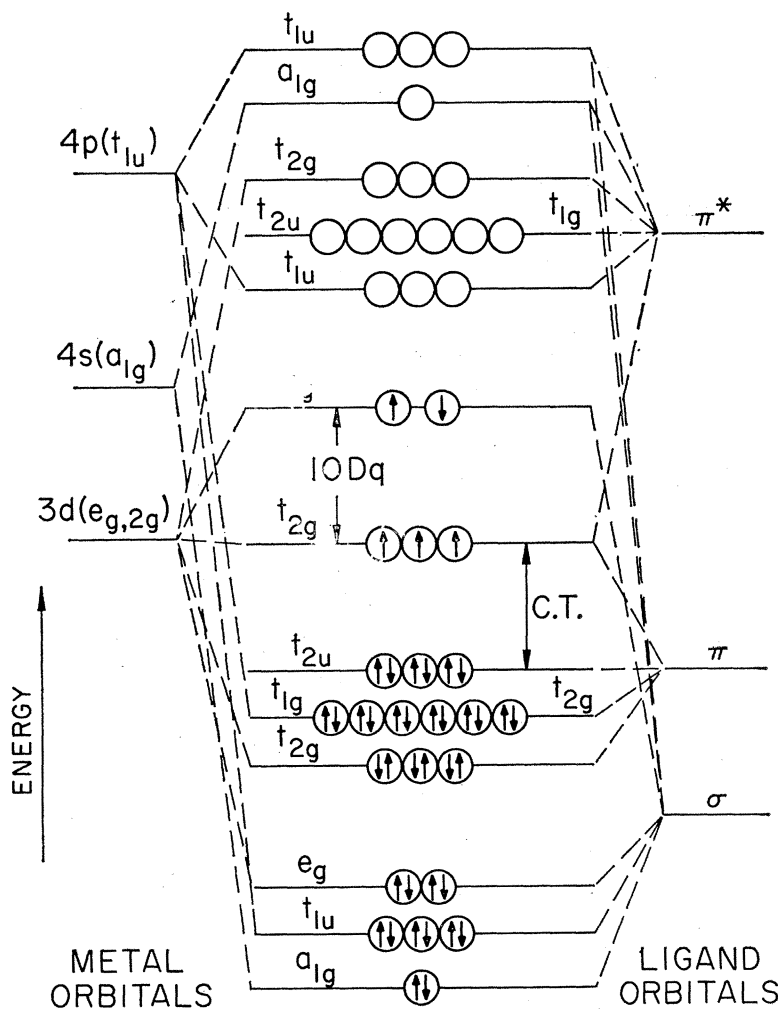


Fig. 1. Molecular orbital diagram—Octahedral symmetry

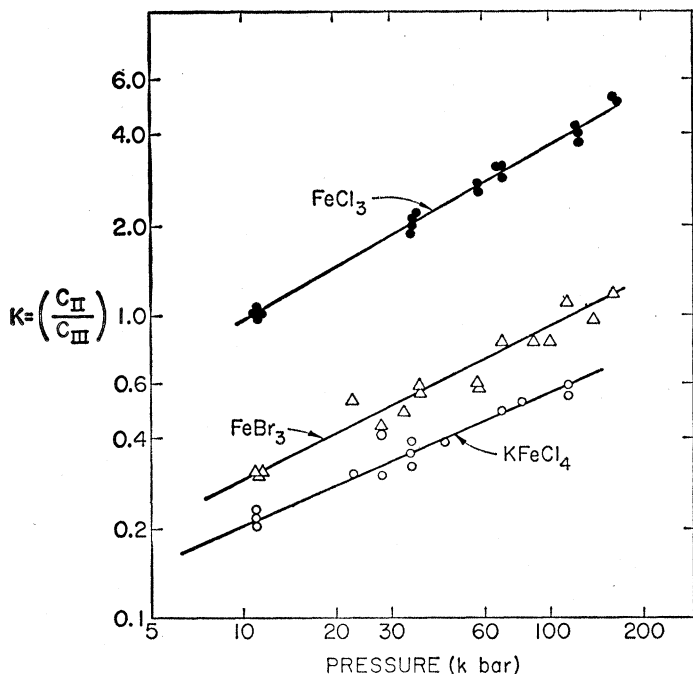


Fig. 2. $\ln K$ vs. $\ln P$ —Ferric halides

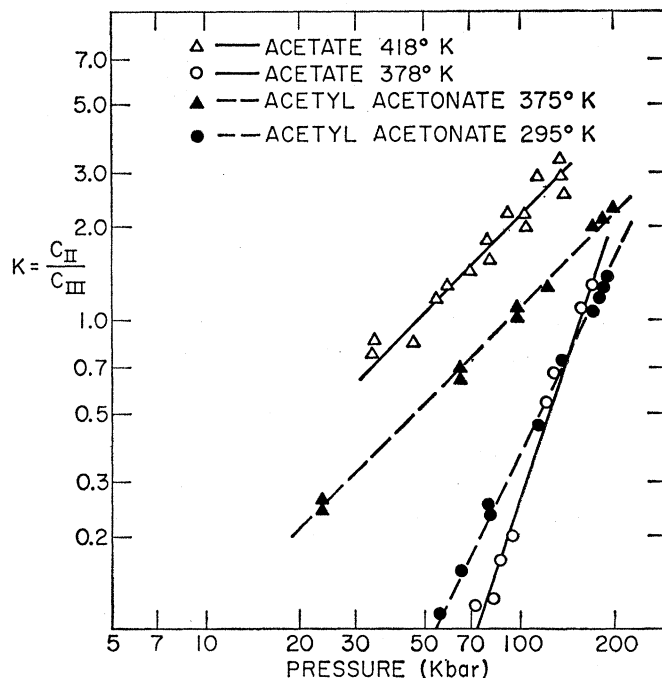


Fig. 3. $\ln K$ vs. $\ln P$ —Acetylacetonate and basic acetate.

much over 90% are difficult to establish accurately, so one cannot say whether this description is applicable at very high dilution. For the halides, as well as for several other compounds which can be classified as relatively ionic, $B \approx 0.5$ with little temperature dependence. This corresponds to values of $\Delta\bar{V}$ which range from about 1.2 cc at 10 kilobars to about 0.06 cc at 200

Table 1. Constants A and B for the relationship $K = AP^B$.

Material	Temperature (°K)	A	B
FeCl ₃	295	0.265	0.564
FeBr ₃	295	0.076	0.426
KFeCl ₄	295	0.091	0.497
FePO ₄	295	0.079	0.457
Fe Citrate	295	0.112	0.350
K ₃ Fe(CN) ₆	295	0.109	2.06
Fe acetylacetonate	295	1.2×10^{-5}	2.23
Fe acetylacetonate	375	0.96×10^{-2}	1.01
Fe basic acetate	378	0.22×10^{-6}	3.05
Fe basic acetate	418	2.21×10^{-2}	0.98
Fe oxalate	295	0.041	0.51
Fe oxalate	335	0.029	0.83
Fe oxalate	383	0.043	1.146
Strontium Fe oxalate	295	0.115	0.301
Strontium Fe oxalate	383	0.058	0.844
FeCl ₃ • 6H ₂ O	294	0.063	0.95
FeF ₃ • 3H ₂ O	294	0.027	0.95
FeF ₃ • 3H ₂ O plus excess H ₂ O	294	0.072	0.95
FeCl ₃ • 6NH ₃ < 25 kbar	294	2.4×10^{-6}	4.06
FeCl ₃ • 6NH ₃ > 25 kbar	294	0.46	0.27
Fe(NCS) ₃ • 6H ₂ O	295	0.136	0.528
K ₃ Fe(NCS) ₆	295	0.024	0.692
Hemin	294	5.5×10^{-3}	1.53
Hemin	335	4.2×10^{-4}	2.04
Hemin	367	3.5×10^{-5}	2.57
Hematin	294	2.7×10^{-5}	2.67
Hematin	343	1.4×10^{-7}	3.77

kilobars. As discussed later, the conversion introduces stresses in the neighborhood of the reduced site. One can insert a term of the form

$$-\sum \epsilon_i \sigma_i$$

in the free energy, where ϵ and σ refer to strains and stresses introduced by the reduction. Then the ΔV of Eq. 2 can be written:

$$\Delta\bar{V} = \Delta V' - \sum \epsilon_i \frac{\partial \sigma_i}{\partial p} \quad (4a)$$

or, in the language of solution theory:

$$\Delta\bar{V} = \Delta V' - \frac{\partial V_e}{\partial C_{II}} \quad (4b)$$

where $\Delta V'$ is the difference in unstrained volumes of the ferric and the ferrous site, and V_e is the excess volume of mixing. Since V_e is strongly concentration dependent, and the concentration of ferrous sites varies with pressure as discussed above, one can understand why ΔV varies with pressure. It can be shown that a small value of B implies a large negative value of

$$\frac{\partial V_e}{\partial C_{II}}$$

at low concentration of ferrous sites (low pressure), and strong coupling between adjacent sites, whereas large B implies weak coupling between adjacent ions or molecules.

Fig. 3 exhibits conversion data for the basic acetate and acetylacetonate

(4). Both of these ligands are bidentate with each molecule attaching to the iron through two oxygens. The values of B , and hence of $\Delta\bar{V}$, are significantly larger here than for the halides, and decrease measurably with increasing temperature. On the other hand, ferric oxalate and strontium ferric oxalate (4) [Sr₃(Fe(C₂O₄)₃)₂•2H₂O] also have bidentate ligands attached through oxygen, but both show an increase of $\Delta\bar{V}$ with temperature (Table 1). It is known that the oxalates reduce photochemically at 1 atmosphere (11, 12) and undergo a series of reactions when

Table 2. Heats of reaction.

Material	Pressure (kbar)	Temperature (°K)	ΔH (eV)
FeCl ₃	*	323	0.12
FeCl ₃	*	393	0.18
FeBr ₃	*	323	0.20
FeBr ₃	*	393	0.32
KFeCl ₄	*	323 - 393	0.07
Fe acetylacetonate	60	325	0.15
Fe acetylacetonate	60	375	0.25
Fe acetylacetonate	150	325	0.065
Fe acetylacetonate	150	375	0.085
Fe basic acetate	75	398	0.93
Fe basic acetate	150	398	0.44
Fe oxalate	25	315	0.19
Fe oxalate	25	360	0.34
Fe oxalate	100	315	0.26
Fe oxalate	100	360	0.42
Strontium Fe oxalate	20	333	0.11
Strontium Fe oxalate	200	333	0.24
Hemin	20	335	-0.22
Hemin	60	335	-0.11
Hemin	90	335	-0.057
Hematin	40	320	-0.23
Hematin	90	320	-0.052

* Independent of pressure

O = Optical transition

T = Thermal transition

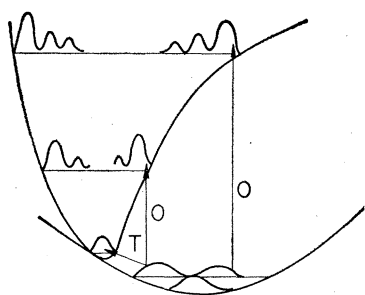


Fig. 4. Schematic configuration coordinate diagram.

heated in the dark (13). In both cases CO_2 is evolved and the process is irreversible. This high pressure process is reversible, and it is not necessary to postulate the formation of CO_2 in the lattice. Nevertheless, the radical formed on reduction may well have a partial molar volume which is quite temperature dependent.

One can obtain a heat of reaction from the relationship:

$$\frac{\partial \ln K}{\partial \frac{1}{T}} = \frac{\Delta H}{R} \quad (5)$$

Values of ΔH are listed in Table 2. In almost all cases the reaction is endothermic. (See the discussion of hemin and hematin below.) The heat of reaction generally increases with increas-

ing temperature. The pressure dependence is, of course, related to the change of B with temperature.

It is possible to give a reasonable discussion of the electron transfer process. The peaks which represent optical transfer of an electron from ligand to metal shift to lower energy with increasing pressure, as discussed earlier in the paper. However, at 10 kilobars this shift represents only a modest fraction of the total energy involved in photoexcitation of the electron. Even at 100 kilobars the shift is only $\frac{1}{3}$ to $\frac{1}{4}$ of the energy difference at 1 atmosphere. One must recognize, however, that the high pressure thermal process may require much less energy than the optical process. Fig. 4 represents a schematic configuration coordinate diagram. The horizontal coordinate is typically a vibrational displacement which aids the electron transfer. By the Franck-Condon principle, optical processes take place vertically on such a diagram. The thermal process is not subject to this restriction. The steep potential well shown for the excited state is consistent with the tail observed for the optical charge transfer peak. Thus, a relatively small vertical displacement of the excited state potential well with respect to the ground state may permit electron transfer.

When the ferric ion at a given site is reduced, a free radical is produced at a ligand site (or a hole may be smeared

out over several ligands). This involves a displacement of charge as well as, quite probably, a physical distortion of the lattice. The combination of strain and electric polarization operating on the neighboring sites distorts the potential wells and reduces the probability of reduction. Further pressure increase lowers the energy of the excited state further and increases the amount of reduction, but at the expense of further strain. These factors must balance out to give the linear relationship observed experimentally. Since $\bar{V}^{\text{III}} - \bar{V}^{\text{II}}$ is positive (Eq. 2) while the Fe(III) ion is smaller than the Fe(II) , there must be a considerable contraction of ligand volume on formation of the free radical.

There are several types of thermal processes involved; the transfer of electrons from ground to excited state, the redistribution in the vibrational levels, and the possible effect of temperature in modifying the shape of the potential wells to relieve or intensify strain. It is not surprising that the heat of reaction is generally dependent on both temperature and pressure. The reduction process is reversible, but frequently involves more or less hysteresis, which can be associated with the mechanical and electrical strains stored in the lattice during the process.

V. Special Cases

In this section we discuss three groups of compounds each of which has aspects of particular interest. In Fig. 5 are presented conversion data for $\text{FeCl}_3 \cdot 6\text{H}_2\text{O}$, $\text{FeF}_3 \cdot 3\text{H}_2\text{O}$, and $\text{FeCl}_3 \cdot 6\text{NH}_3$ (7). For $\text{FeCl}_3 \cdot 6\text{H}_2\text{O}$ it is well established (14) that the iron has four H_2O ligands and two Cl^- ligands. The structures of the other two are not so well resolved, but it is quite certain that they involve some, if not all, molecular ligands. It is seen that the ligand-to-metal electron transfer takes place with these compounds also. The conversion for $\text{FeCl}_3 \cdot 6\text{H}_2\text{O}$ is of the same order as that for the anhydrous material but the value of B (and hence of $\Delta\bar{V}$) is almost twice as large (see Table 1). The $\text{FeF}_3 \cdot 3\text{H}_2\text{O}$ exhibits the same value of B (same $\Delta\bar{V}$) as the hydrated chloride, but a smaller value of A . This compound proved to be very sensitive to H_2O content. The results reported here are for material equilibrated for five months over a saturated CaCl_2 solution. It gave both the correct x-ray pattern and the precise chemical

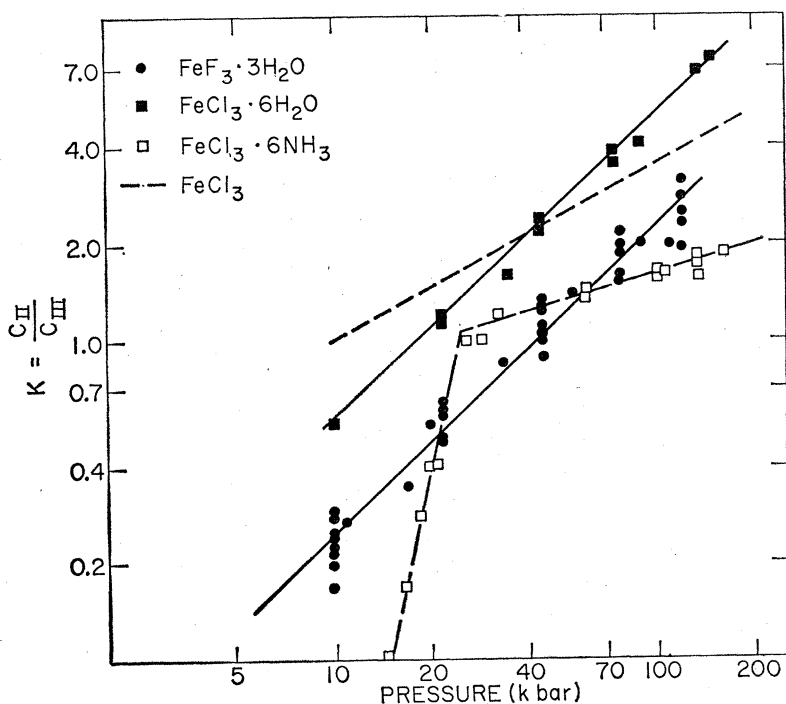


Fig. 5. $\ln K$ vs. $\ln P$ — $\text{FeCl}_3 \cdot 6\text{H}_2\text{O}$, $\text{FeCl}_3 \cdot 6\text{NH}_3$, and $\text{FeF}_3 \cdot 3\text{H}_2\text{O}$

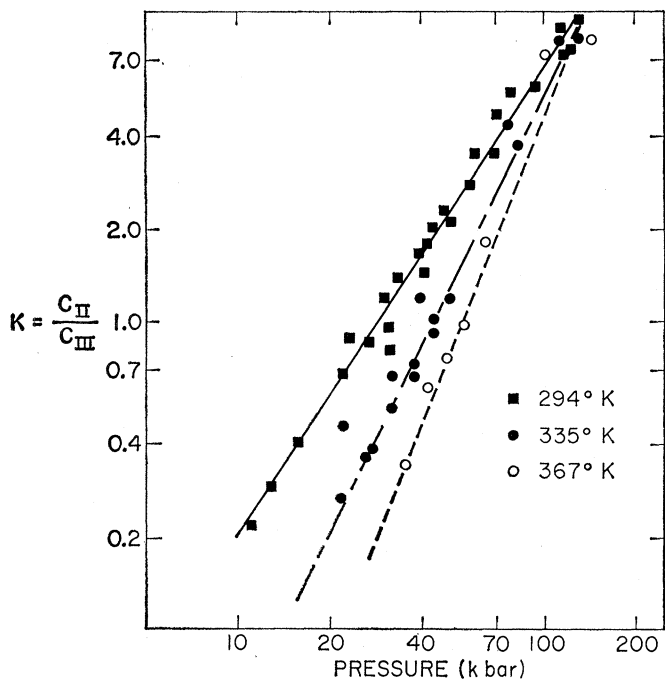


Fig. 6. $\ln K$ vs. $\ln P$ —Hemin

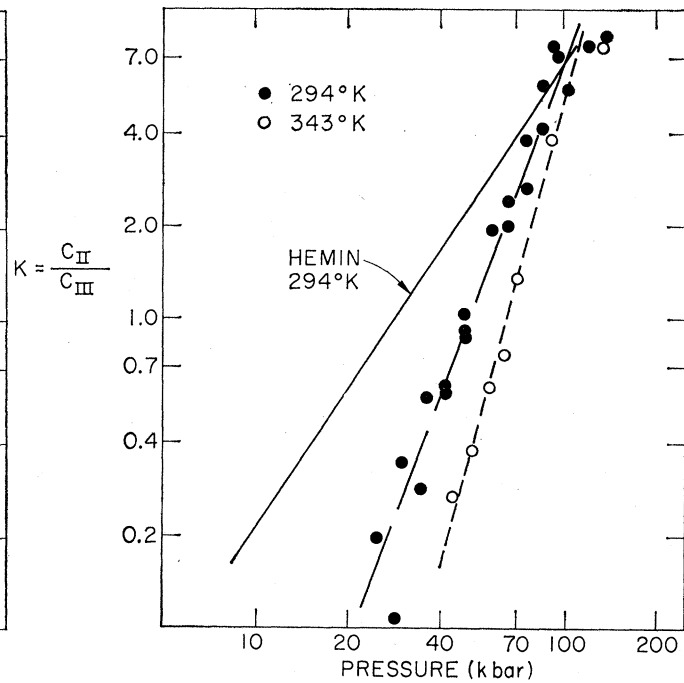


Fig. 7. $\ln K$ vs. $\ln P$ —Hematin

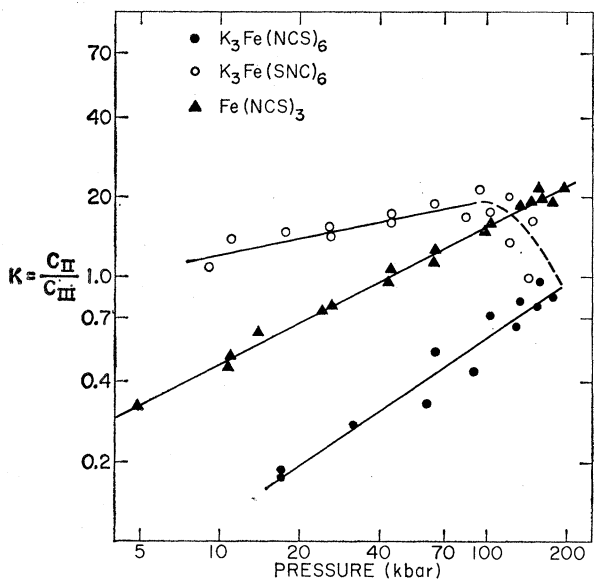


Fig. 8 (above left). $\ln K$ vs. $\ln P$ —Thiocyanate and isothiocyanate.

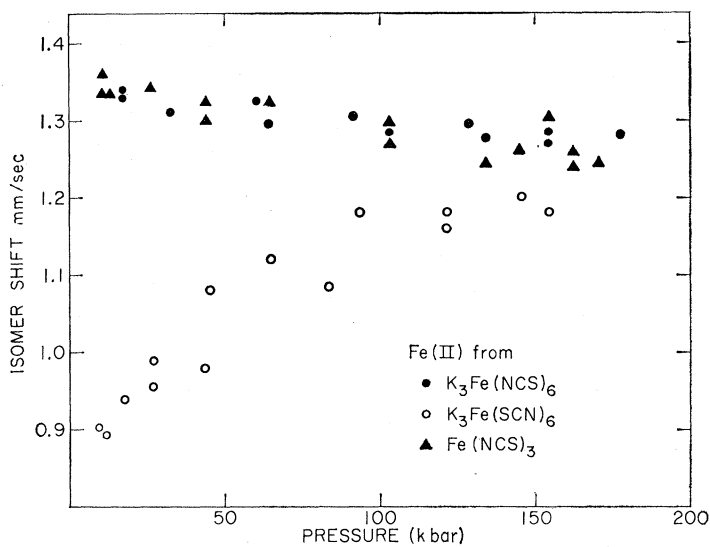


Fig. 9 (above right). Isomer shift vs. pressure—Thiocyanate and isothiocyanate.

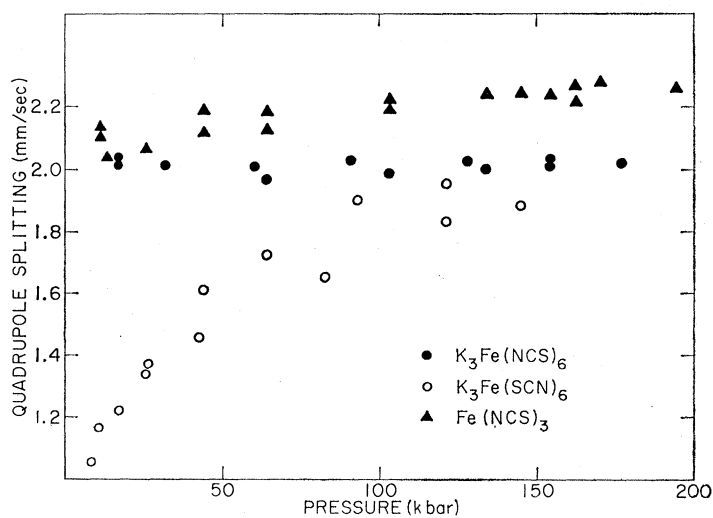


Fig. 10 (bottom right). Quadrupole splitting vs. pressure—Thiocyanate and isothiocyanate.

analysis for $\text{FeF}_3 \cdot 3\text{H}_2\text{O}$. The hydrated ferric fluoride soaked in water just before loading gave the same value of B but higher conversions, very close to those for $\text{FeCl}_3 \cdot 6\text{H}_2\text{O}$. The substitution of D_2O for H_2O made no difference within our accuracy.

The results for $\text{FeCl}_3 \cdot 6\text{NH}_3$ exhibit a new feature. The data can be fitted with two straight lines with a distinct break near 25 kilobars. Orgel (15) has pointed out that in $\text{Co}(\text{NH}_3)_6\text{I}_2$ the optical charge transfer observed is probably from I^- to $\text{Co}(\text{NH}_3)_6^{2+}$. It is possible that for the thermal transfer observed here, in one region the NH_3 to $\text{Fe}(\text{III})$ electron transfer dominates, and in another the Cl^- transfer to the iron-ammonia complex controls.

Hemin and hematin are both prototype molecules for hemoglobin. In both molecules ferric iron is at the center of four pyrrole rings held together by CH_2 groups. Various organic groups attach to the outside of the rings. In the first approximation, iron is in a site of square planar symmetry. In hemin a Cl^- is attached to the ring with the bond perpendicular to the ring. This pulls the iron 0.47 angstrom out of the plane of the organic skeleton. In hematin an OH^- replaces the Cl^- . As can be seen from Fig. 6, hemin reduces with increasing pressure (5) with a rather large value of B . The most surprising feature is the fact that the reaction is exothermic, with a ΔH which decreases rapidly with increasing pressure. Evidently thermal deformation of the potential wells is large and overcomes the effect of thermal promotion of the electron transfer. This deformation is rapidly reduced by increasing pressure. Hematin (Fig. 7) also reduces with increasing pressure in a manner qualitatively similar to hemin. However, the amount of reduction at a given pressure is distinctly less for hematin than for hemin, which indicates that the external ion (Cl^- or OH^-) plays a significant role in the electron transfer process.

Transition metal complexes with the $(\text{SCN})^-$ ion are of considerable interest especially because of the fact that they can attach to the metal either through the sulfur (thiocyanate) or through the nitrogen (isothiocyanate). Generally the first row transition metals

form isothiocyanates, while the heavier metals tend to form thiocyanates. The type of bonding is established from small differences in the infrared spectrum. Burmeister and Basolo (16) have shown that one can obtain thiocyanate-isothiocyanate isomerization in the solid state.

$\text{Fe}(\text{NCS})_3 \cdot 6\text{H}_2\text{O}$ has the isothiocyanate structure. It reduces with increasing pressure (6) in a manner much like a number of rather ionic complexes (see Fig. 8 and Table 1). The ferrous ion formed has an isomer shift (about 1.35 mm/sec) and quadrupole splitting (about 2.1 mm/sec) within the usual range for high spin "ionic" ferrous compounds (see Figs. 9 and 10). The reduction process is reversible, as it is for all the materials discussed above.

On the other hand, the $\text{K}_3\text{Fe}(\text{SCN})_6$ appears to have the thiocyanate arrangement. The isomer shift is within the usual ferric range, but the Mössbauer spectrum is highly asymmetric. The reduction at low pressure is considerably larger than for the $\text{Fe}(\text{NCS})_3 \cdot 6\text{H}_2\text{O}$. The $\text{Fe}(\text{II})$ formed has more nearly the isomer shift and quadrupole splitting characteristic of FeS and FeSe than of typical ionic materials. The amount of $\text{Fe}(\text{II})$ increases slowly with pressure up to about 100 kilobars, then drops off (open circles in Fig. 8). With increasing pressure the isomer shift and quadrupole splitting of the $\text{Fe}(\text{II})$ increase rapidly and approach usual high spin ferrous values (Figs. 9 and 10). Upon release of pressure the $\text{Fe}(\text{II})$ spectrum disappears and one obtains a symmetric $\text{Fe}(\text{III})$ spectrum. If a sample which has been taken to high pressure is reloaded in the cell and subjected to pressure, it shows a symmetric ferric spectrum; and as pressure is increased, a characteristic high spin ferrous spectrum appears. The conversion increases with pressure in a manner very much like other ionic materials (solid circles in Fig. 8). As seen in Figs. 9 and 10, the isomer shift and quadrupole splitting are very similar to the values obtained for $\text{Fe}(\text{NCS})_3 \cdot 6\text{H}_2\text{O}$. The converted material appears to have an isothiocyanate infrared spectrum.

It seems clear that isomerization as well as reduction takes place with in-

creasing pressure, and that the reduction is reversible, but the isomerization is not. There is no tendency for the $\text{Fe}(\text{II})$ peaks to broaden or split as the pressure increases and the isomerization takes place. Apparently, at any one pressure there is essentially only one entity present; i.e. each ion has the same distribution of $(-\text{NCS})^-$ and $(-\text{SCN})^-$ neighbors. The difference in Mössbauer spectrum between ferric thiocyanate and isothiocyanate is sufficiently small that it is difficult to determine to what extent isomerization precedes or follows reduction.

VI. Summary

Ferric ion reduces to the ferrous state with increasing pressure in a reversible manner, with a wide variety of ligands. The phenomenon can be described in terms of changes in the electronic energy levels of the ferric ion vis à vis the ligands, and of strain-induced deformation of the potential wells of the ground and excited electronic states. For one system, pressure-induced isomerization is observed. An understanding of the high pressure chemistry of iron could be significant in biology and geophysics as well as in chemistry and physics.

References and Notes

1. A. R. Champion, R. W. Vaughan, H. G. Drickamer, *J. Chem. Phys.* **47**, 2583 (1967).
2. A. R. Champion and H. G. Drickamer, *ibid.*, p. 2591.
3. G. K. Lewis, Jr., and H. G. Drickamer, *Proc. Nat. Acad. Sci. U.S.* **61**, 414 (1968).
4. S. C. Fung, G. K. Lewis, Jr., H. G. Drickamer, *ibid.*, p. 812.
5. D. C. Grenoble and H. G. Drickamer, *ibid.*, in press.
6. S. C. Fung and H. G. Drickamer, *ibid.*, in press.
7. W. Holzappel and H. G. Drickamer, *J. Chem. Phys.*, in press.
8. H. Frauenfelder, *The Mössbauer Effect* (Benjamin, New York, 1963).
9. G. K. Wertheim, *Mössbauer Effect; Principles and Applications* (Academic Press, New York, 1964).
10. R. W. Vaughan, private communication (1968).
11. W. M. Riggs and C. E. Bricker, *Anal. Chem.* **38**, 897 (1966).
12. N. Saito, H. Sano, T. Tominaga, F. Ambe, *Bull. Phys. Soc. Japan* **38**, 681 (1965).
13. P. K. Gallagher and C. R. Kurkjian, *Inorg. Chem.* **5**, 214 (1966).
14. M. Lind, *J. Chem. Phys.* **47**, 990 (1967).
15. L. E. Orgel, *Quarterly Reviews* **9**, 422 (1954).
16. J. L. Burmeister and F. Basolo, *Inorg. Chem.* **3**, 1587 (1964).
17. The authors wish to acknowledge very helpful conversations and collaboration with R. W. Vaughan, C. P. Slichter, and R. A. Marcus. The research has been supported by the United States Atomic Energy Commission.